CHAPTER - 6

GEOCHEMISTRY

"Geology itself is only chemistry with the element of time added."
Ralph Waldo Emerson

6.1 Introduction

The word *geochemistry* is constituted from two words; *geo* (the Earth) and *chemistry* (branch of science deals with chemical transformation). To understand and quantify the chemical composition, structural property of rocks, a petrologist needs to look for the chemistry of the rock termed as geochemistry. The earth crust has dominantly been made up of primary rock derived from a magma called igneous rocks. The nature of metamorphic rock suits can be broadly defined by major and trace element chemistry. Silicates are the fundamental unit for most metamorphic rocks formed from aggregates of one or more minerals, naturally occurring inorganic chemical compounds. The present chapter embodies the geochemical characteristics of the high-grade gneisses, mafic granulites and pelitic granulites of the study area. It provides a hypothesized model for these rocks' evolutionary history. Geochemical characterization of metamorphic rocks is an essential feature to know petrological evolution of the rocks of the study area. The purpose of the present study is:

(i) Whether the high-grade gneisses and granulites are magmatic/ orthometamorphic or parametamorphic,

(ii) Whether magmatic signatures have been preserved and if so what was the nature of source magma or tectonic environment for magma generation,

(iii) Whether there is an overall signature of depletion of large-ion lithophile element (LILE) and an enhancement of K/Rb ratios, and

(iv) To what extent different granulites are chemically comparable to the Indian granulites province's similar suites.

6.2 Major oxides Geochemistry

The most abundant oxides in metamorphic rocks, which deal with in order of increasing atomic numbers are the oxide of sodium (Na_2O), magnesium (MgO), aluminium (Al_2O_3), silicon (SiO_2), phosphorus (P_2O_5), potassium (K_2O), calcium (CaO), titanium (TiO_2), manganese (MnO) and iron (Fe, both ferric Fe_2O_3 and ferrous FeO). They are mostly used for rock classification and construction of variation diagram. Major elements present in an amount on the earth crust more than 1wt % and trace elements are less than 1 wt %, because the behaviour of the major oxides in magmas can be manifested in terms of differentiation index. Likewise, trace elements behave in the same manner as major elements because they substitute element for major elements. Hence, geochemistry is the most effective tool to discriminate protolith of metamorphic rocks, identify involved magmatic processes, and nature of melt, as well as tectonothermal environment based on quantitative measurement and patterns of geochemical variations. It is fascinating to decide whether the metamorphic rocks' protoliths are of sedimentary or igneous origin, with many discrimination diagrams employed in the literature. In the present context, the discrimination function (DF) derived by [329]:

$$\mathbf{DF = 10.44 - 0.21SiO_2 - 0.32Fe_2O_3(total\ Fe) - 0.98MgO + 0.55CaO + 1.46Na_2O + 0.54K_2O}$$

All the mafic granulites show positive DF values, and therefore, the precursors of the mafic granulites are igneous origin [329].

6.3 Trace Element Geochemistry

Trace element geochemistry has been appreciated for establishing or determining the Earth's evolution, and also used for recognizing their depositional environment. The

comparative abundances of trace elements are broadly recognized for the evolutionary process because they are sensitive to partial melting, crystal fractionation and source composition. The trace element proportion of the melt depends on the parent material, the melting process, the remaining crystal phases after removing the melt, any differentiation before to complete crystallization and any possible interaction with rocks, melts or fluids [185]. The trace elements would provide better tools for understanding the geochemical process than the major oxides. The concentration of these elements (Rb, Sr, Nb, Zr, Ba, Cs, Hf, Ta, Pb, etc.) in rock is less than 0.1% and are expressed in parts per million (ppm), they are used to study elemental distribution in crystal-melt equilibria. Trace elements that have priority in the mineral phase are described as compatible. In contrast, elements that have a melting preference are said to be incompatible [330], based on the charge-size ratio or ionic potential, incompatible elements are categorized into high field strength (HFS) element (Sc, Ta, Y, U, Nb, Pb, Hf) and LILE (Cs, Rb, Ba).

6.4 Rare Earth Elements Geochemistry

The geochemical behaviour of Rare Earth Elements (REE) changes gradually from La to Lu. REE contents of igneous rocks offer significant evidence about the magma source, the degree of partial melting of that source, the degree of crustal contamination, and the quantity of crystal fractionation during magma evolution. REE are normally deliberated to be immobile when post igneous alteration and low-grade metamorphism [185]. REE patterns help understand the magmatic bodies' petrogenesis process and tectonic discriminate setting [331].

REE are a group of 15 (trace) elements with an atomic number from 57 (La) to 71 (Lu), 14 of these elements (except Promethium-Pm) occur naturally. For convenience

the REEs are divided into two sub-groups: (i) La to Sm are denoted to as the light rare earth elements (LREE) and (ii) Gd to Lu are recognized as the heavy rare earth elements (HREE). However, middle rare earth elements (MREE) are applied to the elements from about Sm to Ho [332]. In nature all of the rare earth elements exhibit a 3+ oxidation state (trivalent), except Ce^{4+} (oxidized) and Eu^{2+} (reduced) under most geological conditions.

6.5 Analytical techniques

In the present study, eighteen representative samples from Daltonganj area of the CGGC were chemically analyzed for the major, trace and REEs. The geochemical data of various rocks are given in Tables 6.1-3. To avoid alteration rind, representative samples were collected from the unweathered surface, then powdered using a jaw crusher, pulverization mill and agate mortar. XRF carried out whole-rock major elemental analyses, and trace, REE analysis were carried out by ICP-MS, the details of which are given below. To understand the behavior of major, trace and REEs in different rocks by varieties of diagrams, ratios correlations have been used.

6.5.1 XRF and ICP-MS

XRF (X-Ray Fluorescence) and ICP-MS (Inductive coupled plasma-mass spectrometry) analysis have been done for major oxide, trace and REE. These were carried out at Birbal Sahni Institute of Palaeosciences (BSIP) Lucknow, India. Samples were prepared by the pressed powder method using boric acid as a binder (boric acid: sample ratio, 2:3). Major oxides were analyzed by XRF using wavelength dispersive (WD-XRF AXIOS MAX) machine with power: 4KW, 60kV–160mA analytical, on pressed powder pellet machine used ‘kameyo’ at pressure 15–20 ton, with 4mm pallet thickness. REEs were analyzed by ICP-MS (Make: Agilent, Model: ICP-MS 7700). All

solutions were prepared using ultrapure water (18.2 MX). All the samples were digested by taking 30 mg (300 mesh) sediment powder by using supra pure acid (HF, $HClO_4$, HNO_3) four solutions (10, 40, 100, 200 and 300 ppb for all elements) were prepared by 71A and 71B multi-element calibration standard solutions (Inorganic ventures) as external calibration. The data set will be below 5% error with the right calibration curve.

6.6 Mafic granulite

6.6.1 Major oxides

The compositional variation of the major oxides of the mafic granulites are given; SiO_2 (48.86–48.99 wt%), Al_2O_3 (13.03–14.68 wt%), MgO (4.41–6.93 wt%), Fe_2O_3 (12.57–17.77 wt%), K_2O (0.43–1.74 wt%), TiO_2 (1.07–3.21 wt%), CaO (7.81–9.69 wt%), Na_2O (2.21–2.86 wt%) and P_2O_5 (0.17–0.83 wt%). The analytical data shows that all the mafic granulites are olivine normative with 47 to 50 wt% in silica. The mafic granulite samples show basaltic nature when plotted on the total alkalis vs silica (TAS) plot [182] (Fig.6.1a). Where silica content is between 45–50 wt%, and combined alkali (K_2O + Na_2O) is less than 5%, which corresponds to basalt. The Bivariate diagrams (Fig.6.2) plotted for the major oxides of mafic granulites. Major oxides are plotted against the MgO wt% to reveal magmatic evolution through elemental partitioning. A negative correlation is found between MgO with Fe_2O_3, MnO, and TiO_2, while a positive correlation between MgO with SiO_2, Al_2O_3, and CaO is experienced. During post-crystallization processes, high mobility elements represent scattered data plots of MgO with Na_2O and K_2O. The decrease in Fe_2O_3 and TiO_2 with increasing MgO with the robust negative anomaly of Nb, and Ti, recommends fractionation of Fe-Ti oxides for all the mafic granulite samples.

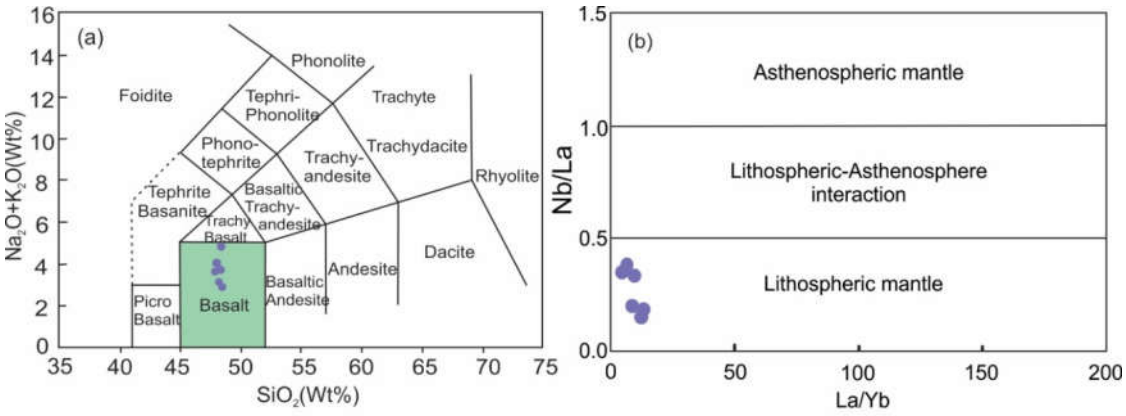

Figure 6.1(a) The chemical classification and nomenclature of volcanic rocks using total alkalis versus silica diagram of mafic granulite (after [182]), (b) La/Yb vs. Nb/La plot (after [333]) ruling out significant Lithospheric contribution in the mantle source region of the Daltonganj mafic granulites.

6.6.2 Trace elements

Trace element data provide valuable information on the rocks' pre-metamorphic parentage because many elements, especially the rare earth element (REE), are believed to be unaffected by regional metamorphism unless partial melting is involved [334]. However, some elements such as Ba, Rb, Sr and LREE are mobile and are not believed to be useful for tectono-magmatic discrimination purpose, therefore, elements such as Ti, Cr, Ni, Fe, Nb, Ta, Zr, Hf, and V, which are comparatively immobile during weathering and metamorphism is used as far as possible. The PM normalized trace elements of the Daltonganj mafic granulites show a negative peak for Ti, K, Nb, Sr and positive peak for U, Ta, and Hf which reveals a rich LILE pattern (Fig.6.3a). High elemental concentrations of Mg, V, Cr, and Co suggest that they be derived from primary magmatic sources [335]. The amount of HFSE (Y, U, Pb, Hf, Nb, Ta) is small, indicating that the rock is derived from the mafic source. Nb has negative anomalies that showed crustal contamination. Besides, mafic granulites have modest Cr, Ni content, Cr values

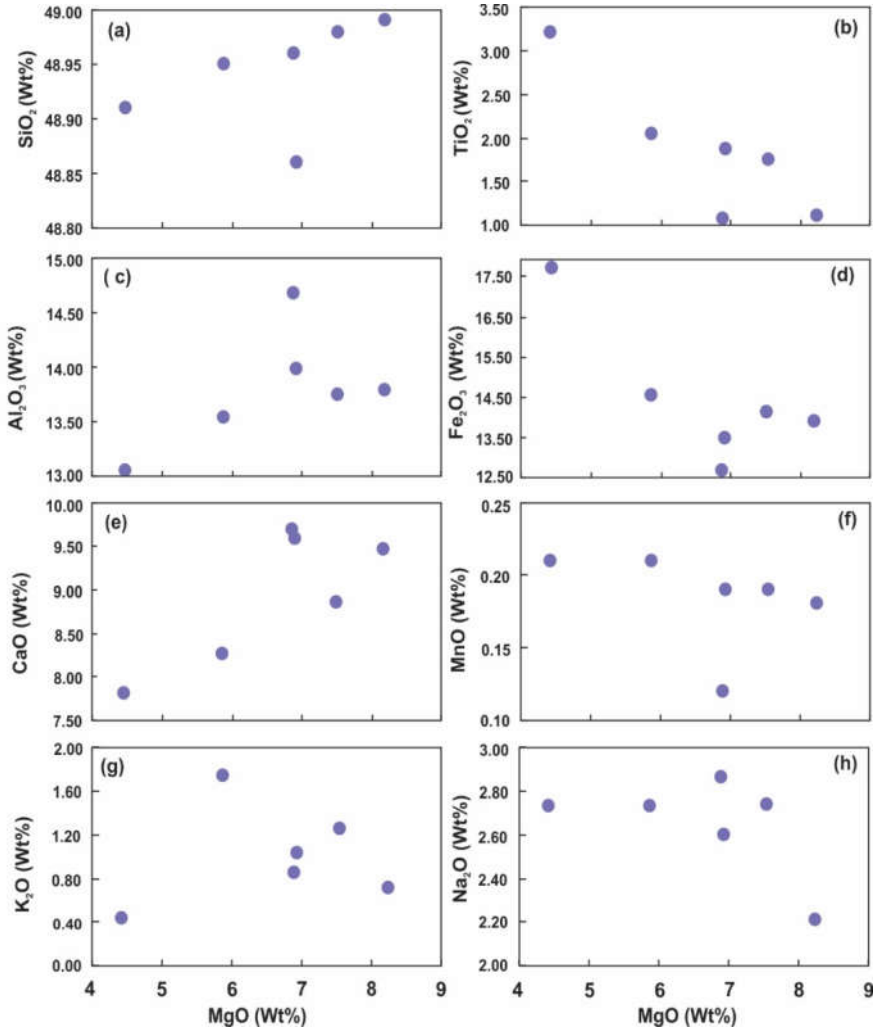

Figure 6.2 Bi-variate plots (oxides in wt%) (a) MgO vs SiO_2, (b) MgO vs TiO_2, (c) MgO vs Al_2O_3, (d) MgO vs Fe_2O_3, (e) MgO vs CaO, (f) MgO vs MnO, (g) MgO vs K_2O, and (h) MgO vs Na_2O for the Daltonganj mafic granulites are showing good fractionation trends except for K_2O and Na_2O.

between 41 ppm and 447 ppm and Ni values between 48.74 ppm and 159.49 ppm and HFSE (high field strength element) ratios as, Nb/Y less than 0.5.

Since the element-element ratios are important in the petrogenesis of magmatic rocks. Notably, K/Rb ratios of the present rocks range from 222 to 891, so the average crustal value is over 250. The Yb-Th discriminant diagram (Fig.6.4a) of mafic granulite shows the calc-alkaline nature [184]. Y-La-Nb discrimination diagram of mafic granulites suggests an orogenic tectonic setting (Fig.6.4b) [336].

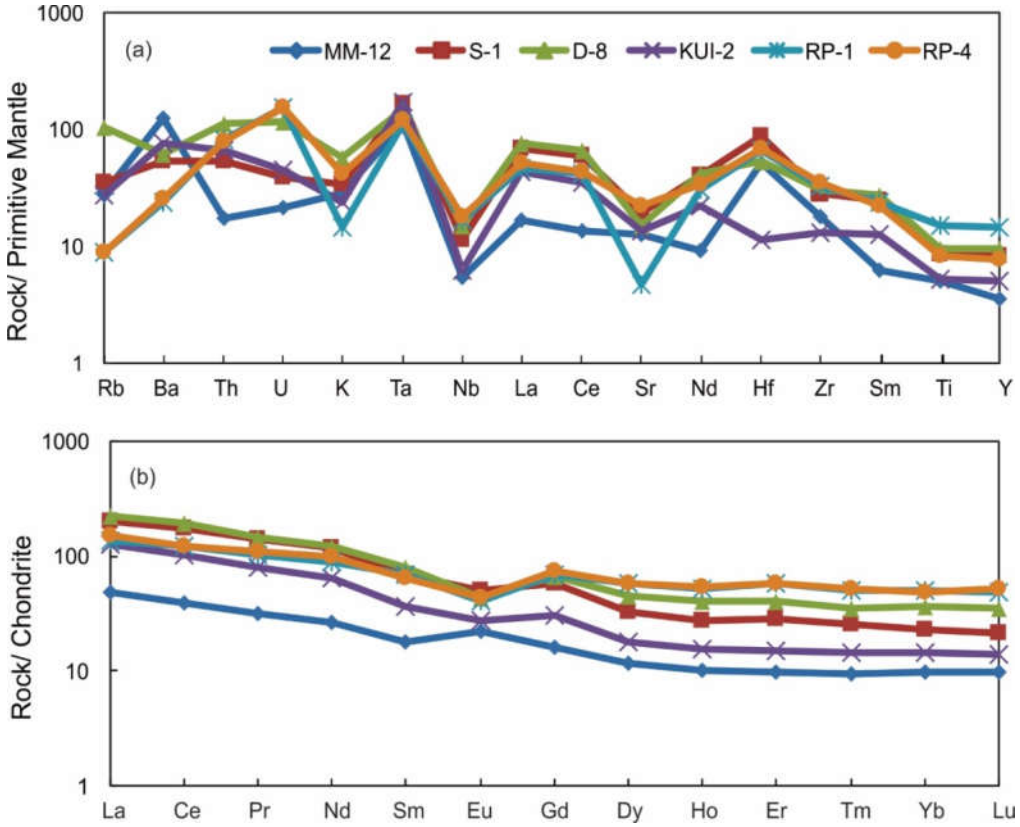

Figure 6.3(a) Primitive mantle [337] normalized multi-element spider diagram for the Daltonganj mafic granulites and (b) Chondrite normalized [337] rare earth element distribution pattern.

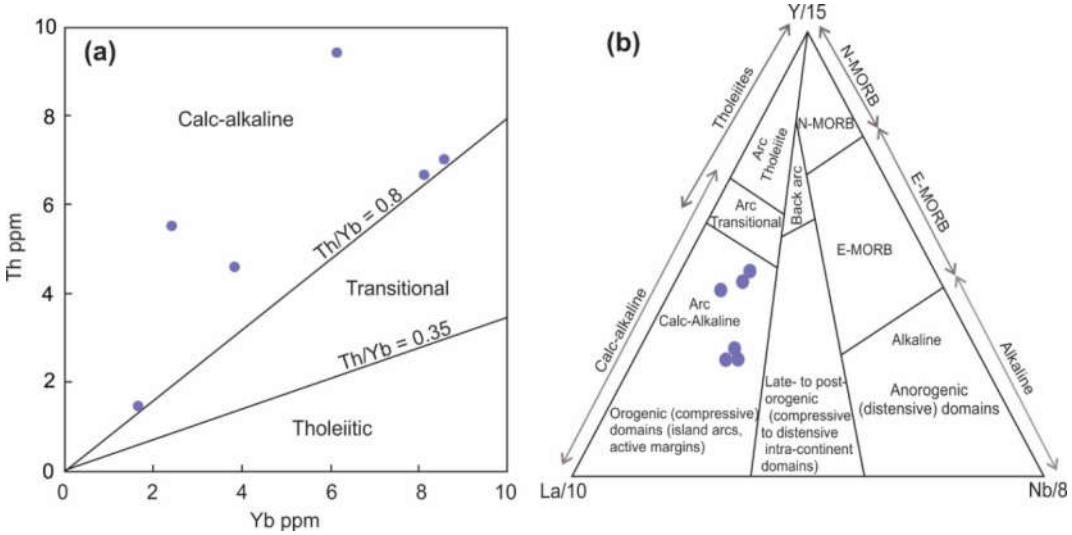

Figure 6.4 Tectonic discrimination diagrams for Dalonganj mafic granulites; (a) Th vs Yb bivariant plot (after [184]), (b) Y-La-Nb ternary diagram (after [336]) illustrating orogenic affinity, and both diagram show all the samples belong to Calc-alkaline nature of basalt.

6.6.3 REEs

REE concentrations are generally normalized to an authentic reference standard, mostly chondritic meteorites' values. Chondritic meteorites were selected as they are considered relatively unfractionated solar system samples dating back to the original nucleosynthesis. To compare graphically, REEs are represented by the spider diagram for the mafic granulites (Fig.6.3b). The Eu anomaly ratio is a measure of [206] and a value more than 1.0 indicates a positive anomaly while a value of lesser than 1.0 is a negative anomaly. The Eu anomalies can be determined by comparing analyzed concentration with a probable concentration projected between the normalized values of Sm and Gd (Eu_N*). The variation of Eu_N/Eu_N* is also limited (0.18 to 0.57), suggesting a source signature rather than feldspar fractionation [338].

The REE distribution patterns (Fig.6.3b) of mafic granulites are slightly enriched in the LREE and show negative Eu anomaly except for the MM-12 sample. The negative Eu anomalies detected may be due to eliminating plagioclase from a melt. Discrete enhancement of HREE is more significant in RP-1 and RP-4 than in other mafic granulite samples. The basalts' sub-parallel REE patterns suggest that compositional variation resulted from crystal fractionation [39]. The degree of fractionation represented by the $(La/Yb)_N$ ratios varies from 0.40 to 2.18, relatively low for these rocks.

6.6.4 Discussion

Several important issues of Daltonganj mafic granulites are discussed based on the current geochemical studies. This discussion is mafically centered on the pre-metamorphic signature of the mafic granulites, nature and differentiation trend of magma, and tectonic environment. One of the important issues relates to granulite facies

metamorphism, i.e., the selective depletion of the mafic granulites during granulite facies metamorphism is also addressed. From the present geochemical study, it is clear that the precursor rocks of the mafic granulites were of magmatic origin; the documentary evidence supporting this view is the positive DF values derived by [329].

6.6.4.1 Petrogenesis

Geochemical composition of sedimentary/metasedimentary rocks plays a crucial role as a sensitive indicator in determining their provenance and to constrain the tectonic setting in which they were deposited, and also to understand the evolutionary development of the early continental crust [195-198, 200, 201, 203-205, 339].

6.6.4.1.a Implications from trace and REEs

The nature of the trace element and the REE pattern progressively suggests protoliths' origin from the magma fractionation [186]. The chondrite-normalized REE patterns of mafic granulites are showing low fractionated REE patterns, and are rich in LREE and relatively low HREE with a negative Eu anomaly (Fig.6.3b). These characteristics may be recognized as the parent rock has plagioclase-rich and garnet free composition. On the Harker diagram, CaO-MgO (Fig.6.2) co-variation requires plagioclase ± clinopyroxene precipitation from the mafic liquid. Mantle peridotite represents the preferred accommodation of LREE in clinopyroxene while HREE within the garnet [188]. The higher abundances of Rb, Ba, U, Pb and LREE in mafic granulites are interpreted as a result of a rich component of the fluid [191]. Th, U, and Pb exist as high concentrations within the basaltic protolith, indicating crustal components' involvement at their origin. Nb and Ti are a negative anomaly and are observed to be characteristics of the subduction-related environment. The relative abundance of REE in

igneous and metamorphic rocks is generally considered a useful indicator of tectono-magmatic affinity. The characteristic flat to depleted REE content as reflected from the present samples are assumed to be the melt from the primitive mantle with little or no enrichment to deplete the LREE relative to the HREE .

6.6.4.1.b Mantle source and subduction zone enrichment

It is known that the present mafic granulites are predominantly tholeiitic with olivine normative and thus suggest one of their mantle sources underwent shallow and hydrous melting. This mantle-derived magma's crustal contamination is one of the crucial issues for mafic granulites. Several geochemical parameters can be used to evaluate the problem of mafic magma contamination by continental crust, and the following is a discussion of their application to this magma composition of rocks. Intermediate composition of SiO_2 (<49 wt %) with a low U (0.44–3.26 ppm), Th (1.45–9.40 ppm) and Pb (7.47–11.55 ppm) suggests that magma arises from bulk-assimilation of continental crust. Th/La ratio (>0.12) indicates potential crustal contamination during the emplacement of mafic magma [337]. The negative anomaly of HFSE is demarcated as subduction-related magmatism, and it also supports HFSE elements present in the Ti-bearing remaining phases within mantle-derived magma. Mantle-derived magma is also identified by the HFSE/LREE proxy [333] and Nb/La (< 0.37) ratio, which is lower for the Daltonganj basaltic protolith and represents the provenance of the lithospheric mantle (Fig.6.1b). The Nb/U versus Nb discrimination diagram [340] for the mafic granulites is lower than the MORB and OIB (Nb/U ~ 25), which refers to the melt phase originating from the subducted slab and being metasomatized from the mantle source (Fig.6.5a). The subduction influenced source is also sustained by high Th/Yb and low Nb/Yb content;

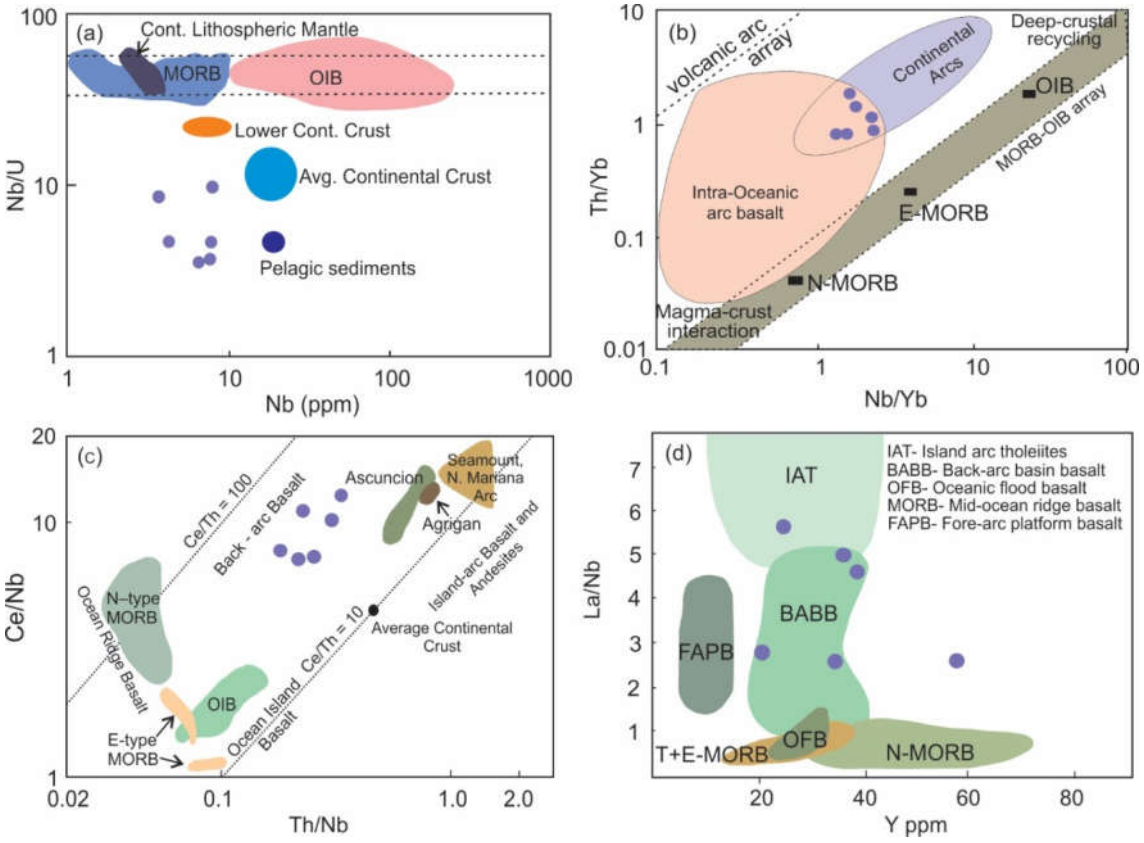

Figure 6.5(a) Nb (ppm) vs Nb/U plot ([340] and references therein), (b) Th/Yb vs Nb/Yb diagram [341] depicting a subduction-related enrichment for the Daltonganj mafic granulites samples. Fields for intra-oceanic arc basalt is from [342] and reference therein. (c) Th/Nb vs Ce/Nb (after [343], and (d) Y vs La/Nb diagram (after [344], N-MORB: normal mid-ocean ridge basalt. E-MORB: enriched mid-ocean ridge basalt. OIB: ocean island basalt.

these rock data are beyond the MORB-OIB array in field of intra-oceanic arc basalt (Fig.6.5b). High Th/Yb and low Nb/Yb values have indicated that basaltic magma was a subducted-slab product derived from the mantle source (Fig.6.5b). Basaltic magma of the Daltonganj, in Th/Ce and Y-La/Nb discrimination diagrams (Figs.6.5c&d), indicates a back-arc basaltic affinity.

6.7 Pelitic granulite

The status of the pelitic granulites of the present area has been tested by calculating their values according to DF [329], and they are found to be pure of sedimentary origin. These rocks have SiO_2 from 51.26 wt% to 61.64 wt%, high Al_2O_3 contents (14.6 wt% to 19.39 wt%) and relatively low FeO contents and low values of K_2O. The MgO/FeO+ MgO ratio is between 0.11 and 0.28.

6.7.1 Whole-rock geochemistry

A total of seven pelitic granulite samples have been analyzed. The LOI-contain (Loss of ignition) ranges from 1.39 to 3.91. SiO_2 composition exhibits a wide variation (51.26-64.37 wt%), the total alkali-silica (TAS, [345]) diagrams (Fig.6.6a) of pelitic granulites display diorite and monzonite. In contrast, few samples are gabbroic; the pelitic granulite protolith was formed from various sedimentary provenances. All samples have a ferroan character (Fig.6.6b), and most samples are peraluminous with one sample is metaluminous (A/CNK= 0.88-1.39) (Fig.6.6c). However, these are calc-alkalic to alkali-calcic variable composition, but a sample has the calcic composition (Fig.6.6d). Na_2O vs K_2O diagram (Fig.6.6e) represents shoshonitic and ultra-potassic composition, but the SiO_2 vs K_2O diagram (Fig.6.6f) clarifies that all the samples are of shoshonitic nature.

6.7.2 Trace and rare earth element patterns

The trace element spider-diagram with normalization of the primitive mantle of pelitic granulites defines positive anomaly for Ba, Th, K, Pb, Nd, Hf, Sm and Y whereas LILE (Rb, Sr) and HFSE (Nb, Ti) has negative anomaly (Fig.6.7a). Three samples represent minor negative Eu anomalies, and four represent positive anomalies (Fig.6.7b).

Samples D-3 and D-7 exhibit a highly fractionated LREE patterns with low and unfractionated HREE pattern; it looks like a flat pattern. These samples show a relatively high fractionation rate where the $(La/Lu)_N$ ratios vary from 6.2 to 91.2.

6.7.3 Discussion

The geochemical data of pelitic granulites show their unusual composition because they do not correspond to any normal igneous or sedimentary rocks. The mineral of the pelitic granulites' total composition suggests that they were derived from argillaceous parent rocks. However, no undesirable sedimentary structures have survived due to the rocks' recrystallization and reconstitution. Generally, the element's movement is reported between the coexisting mineral phases, so few elements tend to migrate from the crystal phase to the melt phase during metamorphism. Low TiO_2 and high Al, K, Si content reveal granitic rich sediments dominated the pelitic provenance. Some sedimentary significance has also been observed such as enrichment of ∑REE (169.3 to 1586.97 ppm), which may be due to accumulation of immobile elements during sedimentation. Pelitic granulites contain a good amount of Ba and Rb, as the feldspar is an essential mineral for hosting Ba and Rb in terrigenous sedimentary rocks. Moreover, the analyzed geochemical data indicate that pelitic granulites are probably redeposit, and metamorphosed products of Paleoproterozoic weathered crusts.

6.7.3.1 Tectonic implications

After establishing the relationship between the $(Y/Nb)_N$ vs $(Th/Nb)_N$ diagram [346], it has been used to establish the discrimination between oceanic islands, continental crust and convergent margin rocks, and all samples are located in the convergent margin rocks field (Fig.6.8a). The Zr vs Nb/Zr diagram (Fig.6.8b) confined that protolith of pelitic

granulites encountered a subduction-related tectonic setting [347]. The Y vs Nb and Rb vs (Y+Nb) tectonic discrimination diagram shows that the protolith has an affinity towards the within plate granite (WPG) (Fig.6.8c,d) [348]. The Gaya region of

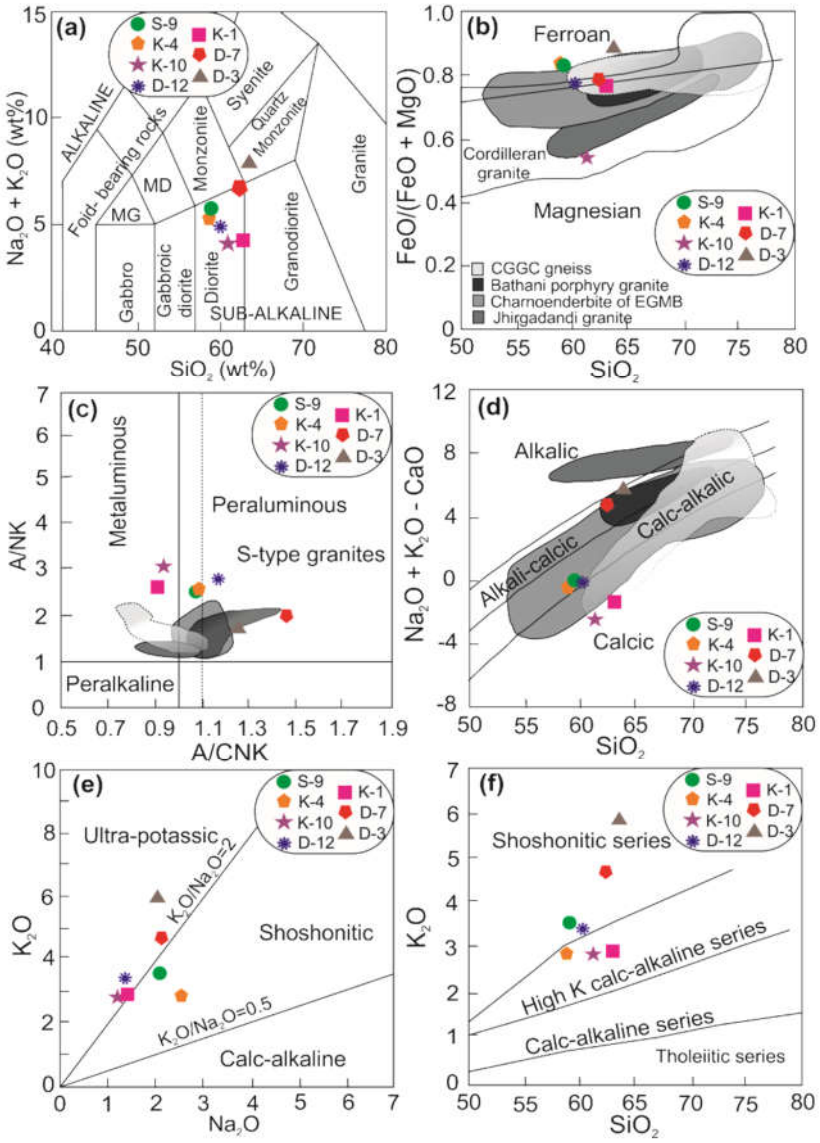

Figure 6.6(a) Total alkali silica diagram after Middlemost (1994). (b-c) Granitoid classification scheme by [349] revealing (b) magnesian to ferroan, (c) slightly peraluminous nature of the studied rock (d) calc-alkalic to alkali-calcic. Field of the Cordilleran granites is plotted after [349]. The data also compared with Bathani porphyritic granite [253], Charno-enderbite of Eastern Ghats Mobile Belt [350], Jhirgadandi Granite [26], Augen gneiss of Dumka from CGGC [266]. (e) Na_2O vs K_2O diagram (after [351]; (f) K_2O vs SiO_2 plot after [352] showing the shoshonitic nature of the rock.

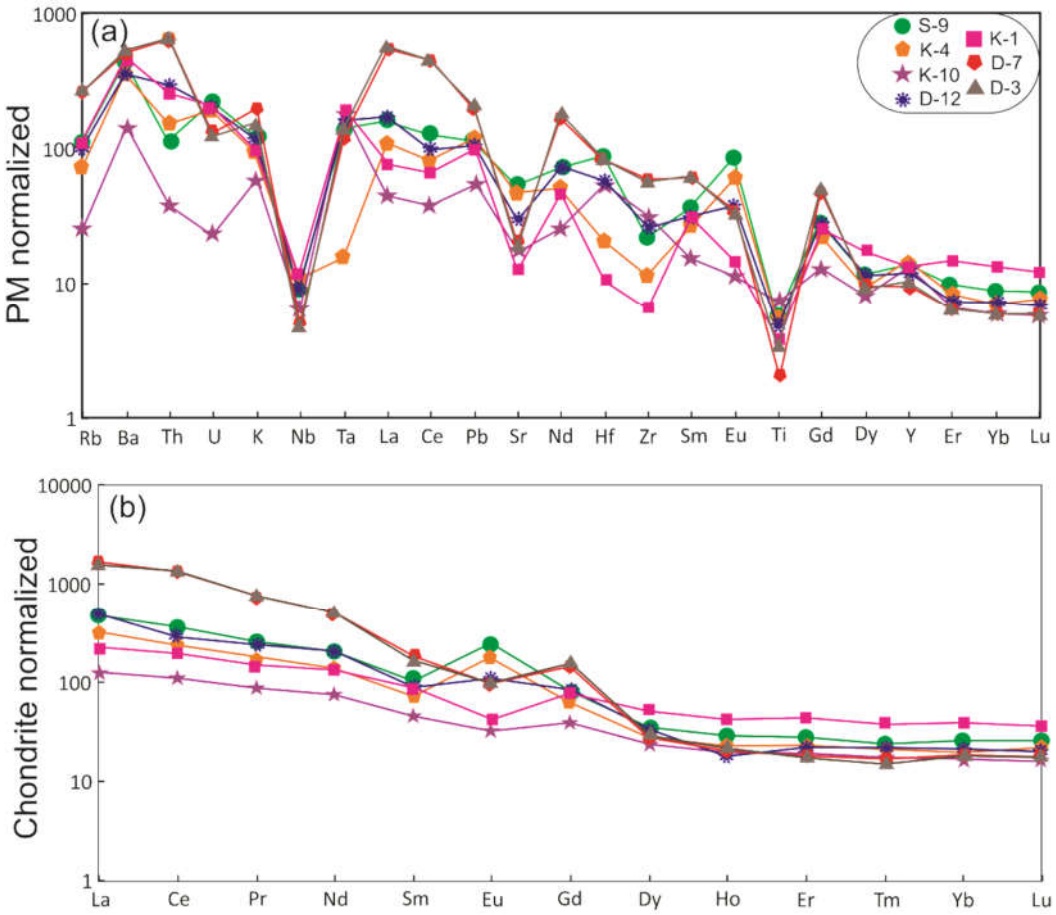

Figure 6.7(a) Primitive mantle normalized multi-elements spider diagram of granulite gneiss after [337]. (b) Chondrite normalized REE plot after [337] showing uniform and nearly smooth REE pattern.

Mahakoshal Mobile Belt (MMB) demarcates tectonic affinity similar to the within-plate granite setting (Fig.6.8c,d) and continental margin magmatic rocks (fig.6.8a) for pelitic granulites [4,353]. The positive anomaly of Pb and negative anomaly of Nb were demarcated on the spider diagram, which suggested that the protolith of pelitic granulites develop during the collisional tectonic setting. The enrichment of K, Th, U, Pb, and ΣHREE and depletion in Nb, Sr, Ti of the studied rocks are significantly involved with the mid-upper crust or subduction-related generation of their protolith [6, 354], a similar trend was also found from the MSB granite during ~1800 and ~1700 Ma age. However, detrital zircon of study area has the same age as the MSB, it was

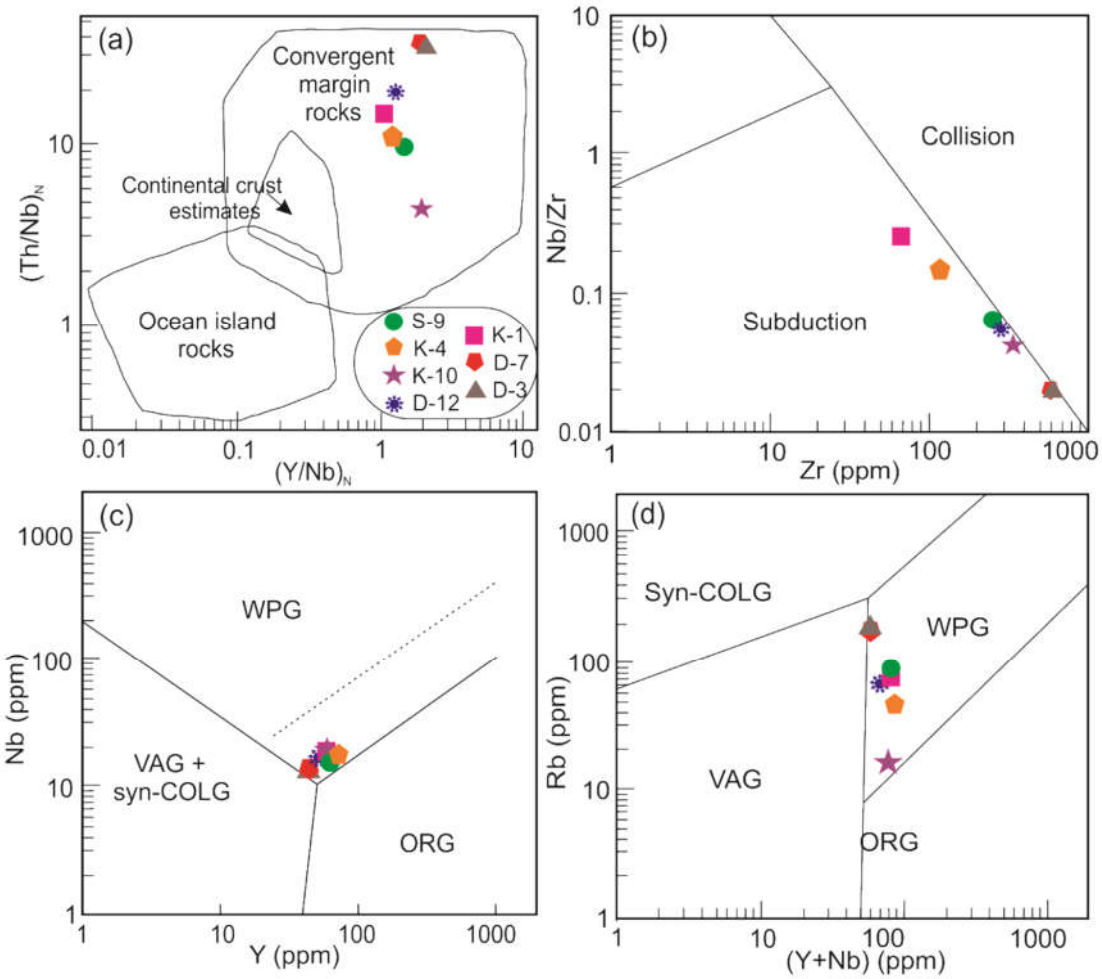

Figure 6.8. (a) $(Y/Nb)_N$ vs $(Th/Nb)_N$ [346] used to discriminate tectonic regimes of granulite gneiss from the Daltonganj of north-west CGGC. (b) Zr vs Nb/Zr plot with fields from [347] showing subduction tectonic regime for the genesis of protolith of politic granulites, (c) Y vs Nb tectonic discrimination diagram (after [348] plotted with granulite gneiss mostly showing an affinity towards the within-plate granite (WPG). (d) Y+Nb vs Rb tectonic discrimination diagram plotted for granulite gneiss. Syn-COLG: syn-collisional granite; WPG: within plate granite; VAG: volcanic arc granite; ORG: ocean ridge granite [348].

considered for the MMB and other terrains that were the source of sediments of pelitic granulites of the CGGC. All these interpretations provide consolidated evidence that pelitic granulites' protolith must have come from the MSB.

6.8 High-grade gneiss

6.8.1 Major oxides

Two types of high-grade gneiss; gneisses garnet-cordierite-amphibole gneisses (D7b, D8a and R-91-96) and garnet-orthopyroxene-amphibole gneisses (K4a and R-91-97) have been taken for geochemical analysis. The major oxides of garnet-orthopyroxene-amphibole gneisses contain more SiO_2 (54.87-55.46 wt%), Al_2O_3 (14.58-14.91 wt%) and CaO (2.54-2.80 wt%) than garnet-cordierite-amphibole gneisses, but are lower in Fe_2O_3 (10.86-11.26 wt%) and MgO (9.71-10.89 wt%), whereas both gneisses have lower amounts of Na_2O (0.28-0.81 wt%), K_2O (0.63-0.98 wt%), and TiO_2 (0.31-0.90 wt%). The gneisses are classified based on total alkali vs silica (TAS) plot [182] (Fig.6.9), on this classification scheme, all of the garnet-cordierite-amphibole gneisses lie in the basalt field, and the remaining two garnet-orthopyroxene- amphibole gneisses

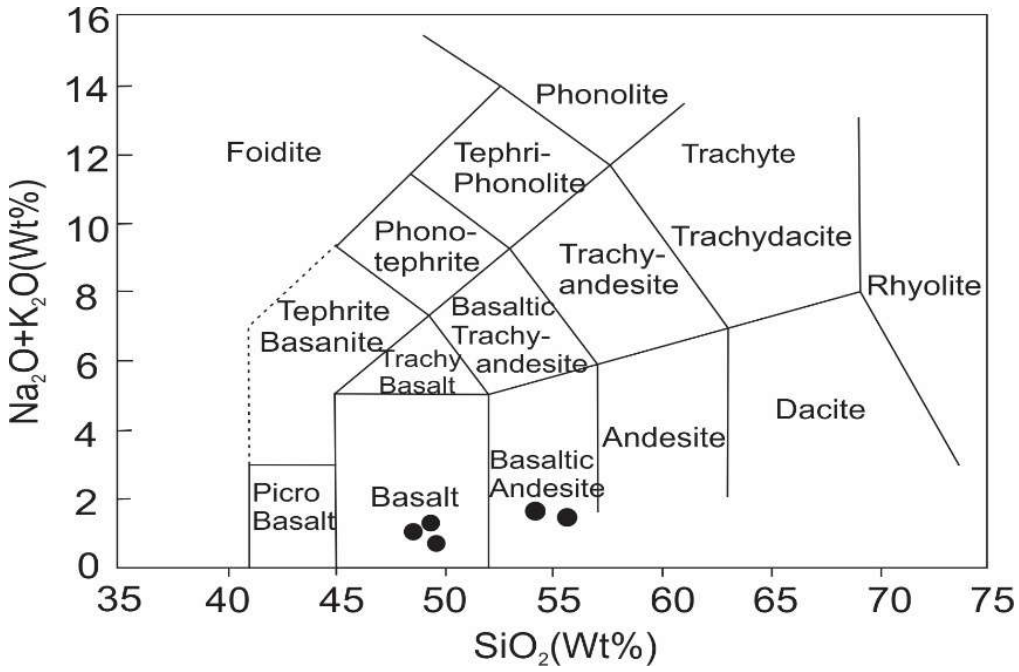

Figure 6.9. The chemical classification and nomenclature of volcanic rocks using total alkalis versus silica diagram of high-grade gneiss.

fall in the basaltic andesite field. In the bivariate plot, a negative correlation is established by MgO with SiO_2, Al_2O_3, TiO_2, P_2O_5, and K_2O; however, a positive correlation between MgO with Fe_2O_3 and CaO is observed for these high-grade gneissic samples (Fig.6.10). The scattering of the data is shown in the MgO and Na_2O plot, presumably influencing this element's mobile nature during the post-crystallisation processes. Bivariate plots indicate that the post-crystallisation secondary process does not affect the studied gneisses' major oxides.

6.8.2 Trace and rare earth elements

The garnet-cordierite-amphibole gneisses are enriched with compatible elements such as (in ppm), Cr (257.29–280.16, Ni (88.23–95.61), Co (52.14–59.62), V (330.21–340.12) and depleted in incompatible elements Rb (14.56–16.24), U (0.45–0.51), Th (3.21–3.52) and Nb (4.59–5.13), while garnet-orthopyroxene-amphibole gneisses are indicating a different trend. The PM normalized HGG rocks pattern (Fig.6.11a) exhibits enrichment in LILE, Pb and Ta, as compared HFSE. Depletion in HFSE is accompanied with a negative anomaly of Nb, Sr, and Ti, whereas the enrichment of LILE with a positive anomaly of Th, Hf, Ta, Pb and Y is a characteristic signature of subduction orogeny. An island arc setting has been validated by a decrease in Nb and Ti concentration. The enrichment of LREE and Th in the studied HGG indicates monazite minerals' availability, and monazite acts as a sink for LREE [355].

The chondrite normalised REE patterns (Fig.6.11b) for gneisses can be classified into two groups; garnet-cordierite-amphibole gneisses show the enrichment of LREE against HREE (La_N/Yb_N = 7.24–9.0) with a slight negative Eu anomaly (Eu_N/Eu_N^* = 0.72–0.80), and garnet-orthopyroxene-amphibole gneisses have also enriched LREE

(La_N/Yb_N=15.88–17.90) with a positive Eu anomaly (Eu_N/Eu_N^* = 2.82–2.91). The subparallel REE pattern suggests that the crystal fractionation was dominated during a phase of compositional variation. The Y-La-Nb plot and Yb-Th discrimination diagram (Fig.6.12a,b) are used to explore the basaltic nature as a protolith of high-grade gneiss.

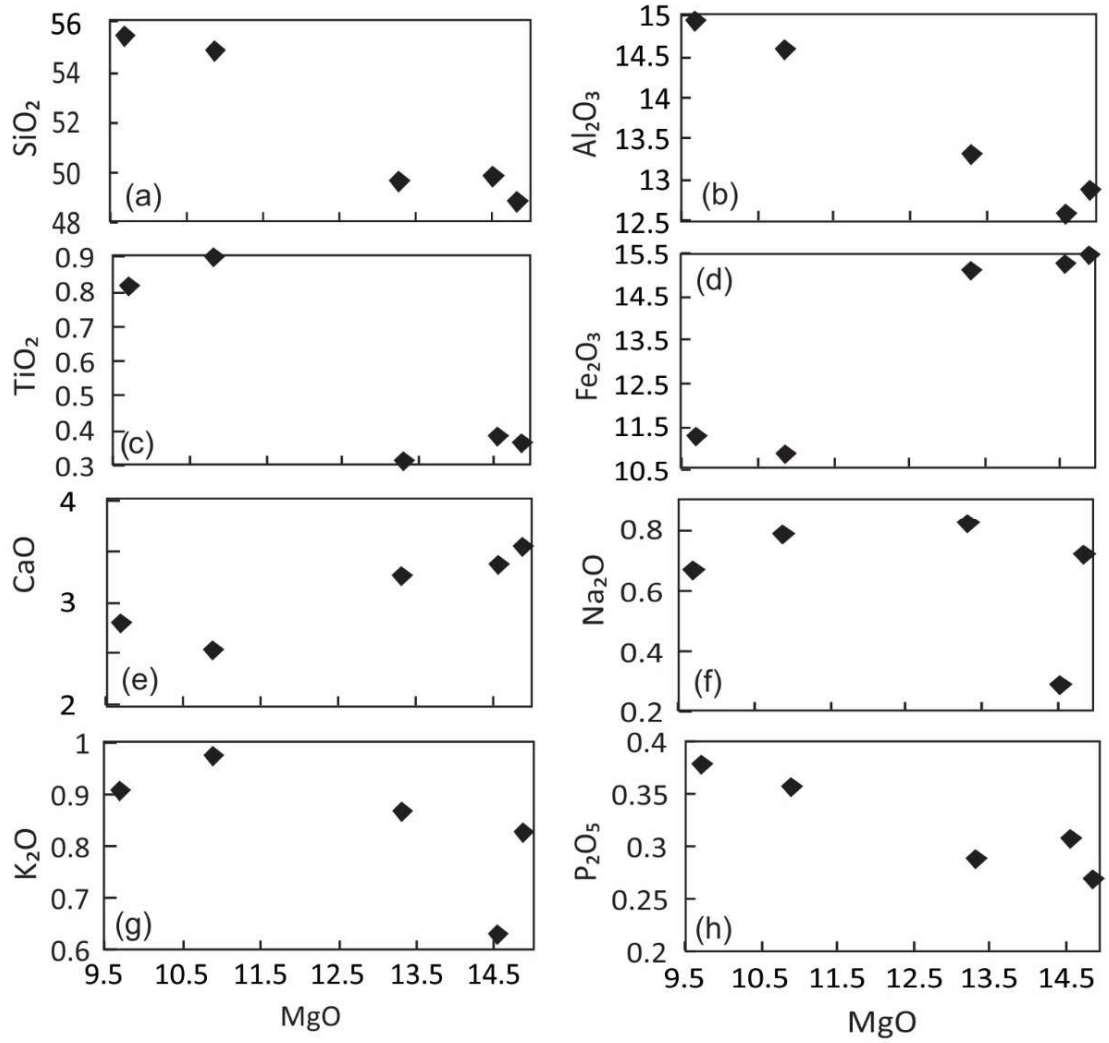

Figure 6.10. Bi-variate plots (in wt%) (a) MgO vs SiO_2, (b) MgO vs Al_2O_3, (c) MgO vs TiO_2, (d) MgO vs Fe_2O_3, (e) MgO vs CaO, (f) MgO vs Na_2O, (g) MgO vs K_2O, and (h) MgO vs P_2O_5.

6.8.3 Geochemical significance

The study area's gneisses have the following problems; (a) Nature of protolith, (b) Causes of strange composition, i.e. high wt% of FeO, MgO, and low in CaO, Na_2O and

K_2O. The following reasons have been endorsed to the high content of FeO and MgO: (1) Metasomatic introduction of FeO and MgO and further removal of CaO, Na_2O and K_2O simultaneously, (2) Removal of the granitic composition from the pre-existing rock during the process of differential anatexis has resulted in the relative enrichment of FeO and MgO. If the felsic melt is removed from the parent rock undergoing anatexis process, a relative enrichment of Al, Fe and Mg and depletion of Na, Ca, and Si may

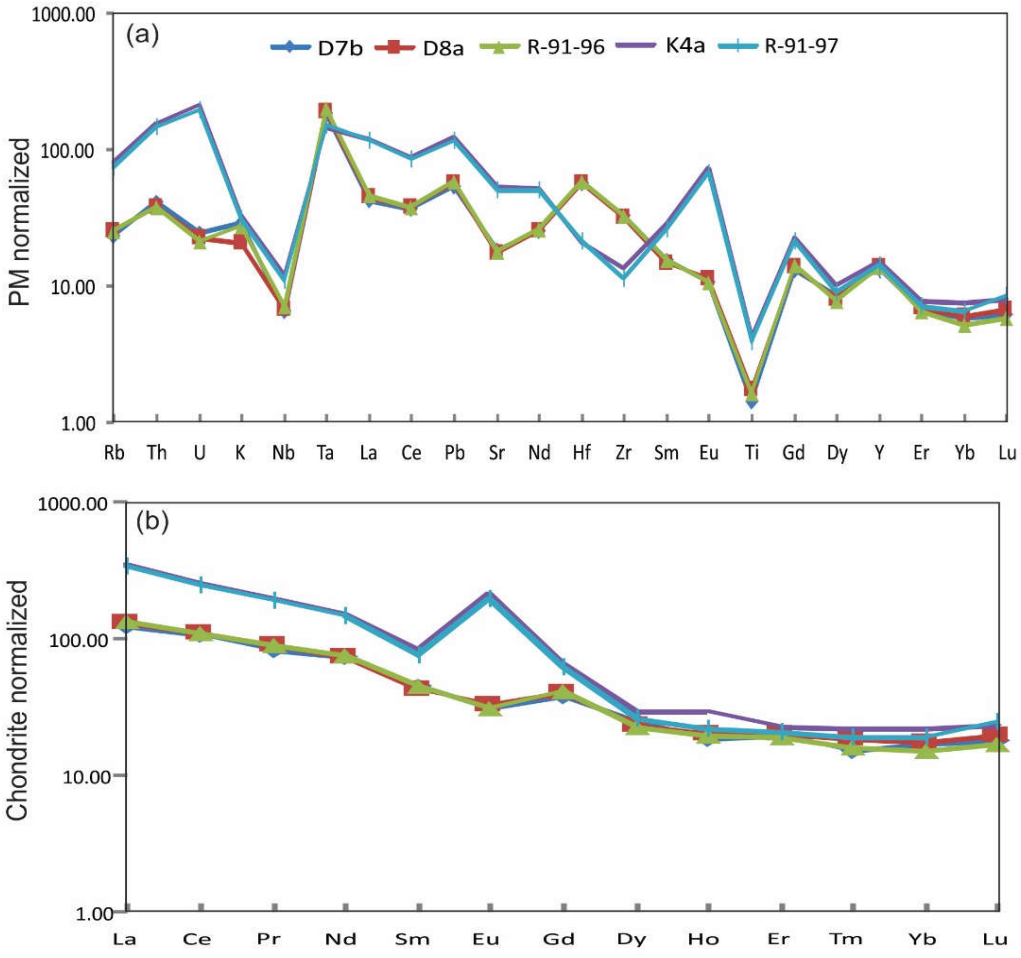

Figure 6.11(a) Primitive mantle [337] normalised multi-element spider diagram for the high-grade gneiss and (b) Chondrite normalised [337] rare earth element distribution pattern.

occur in 'restite'. Decreasing SiO_2, K_2O, Na_2O and CaO have a general tendency while MgO, FeO, and Al_2O_3 increase in these gneisses from granite. It corresponds to relative

enrichment due to the removal of melt of the granite composition. The removal of granitic melt during anatexis process does not significantly affect the X_{Mg} of the 'restites' than the parent rock. The textual study provides evidence of the following reaction by which melt has been formed in the garnet-orthopyroxene-amphibole gneisses from the investigated area.

(a) Garnet + biotite + H_2O → amphibole + cordierite + quartz + melt (6.1)

(b) Biotite + quartz → orthopyroxene + amphibole + H_2O (6.2)

Plagioclase and K-feldspar are absent in these gneisses, but minor quartz are present. It suggests that these gneisses are formed by 'restitic' origin after eliminating granitic melts. Both gneisses show trails of biotite within cordierite and orthopyroxene (Fig.4.1k) and corroded garnet and biotite within amphibole (Fig.4.1i) give the evidence of reaction (6.2) and (6.1) respectively. Therefore, it has been proposed from the above discussion that both gneisses of the Daltonganj area are of 'restites' origin.

6.8.4 Petrogenesis

The crustal material will increase the K_2O and Na_2O chemical composition in the melt after crustal contamination. The studied gneisses have a low content of K_2O (0.63–0.98 wt%) and Na_2O (0.28–0.81 wt%); therefore, there is no chance for any crustal contamination. Similarly, LILE's coherent variation, HFSE and REE patterns ignore crustal contamination [356]. Low HREE content and positive Eu anomaly and negative Sr anomaly have also been reported against the crustal assimilation. The garnet-orthopyroxene-amphibole gneiss represents a more enriched value of LREE than HREE, which means that orthopyroxene's availability behaves as a sink of LREEs. Gneisses have less compatible trace elements that suggest an essential process as fractional

differentiation in their evolution. Here, it is observed that the compatible element's excellent availability (Cr, Ni, Co, V) and low TiO_2 suggests a mafic source rock or may be more possibility of mantle origin. The substantial depletion of K and Na is most pronounced if their protoliths are considered the mafic metavolcanic. Negative Nb and Sr anomalies suggest involvement of subduction setting [341]. Y-La-Nb triangular plot and Yb-Th discrimination diagram (Figs.6.12a,b) indicate the calc-alkaline basaltic nature of these gneisses developed at the island arc domain during subduction-related processes. The enhanced abundance of LREE and LILE (Th, Ta, U, Pb) is better interpreted due to enrichment by fluid-related metasomatism [191]. It is concluded that calc-alkaline rich mafic fluids intruded in the pre-existing rocks, and then emit its mafic components (Fe, Mg). In the process, the modal availability of felsic component of pre-existing rocks decreases, and it signifies a ‘restitic’ origin of the studied gneisses. Because of rocks' susceptibility, pelitic compositions to chemical signatures like high MgO, a restite origin is possible. It is pertinent to mention that the average K/Rb ratios are above 500 and such a high value indicates that the gneissic rock may be of restitic origin after the partial melting event during regional metamorphism.

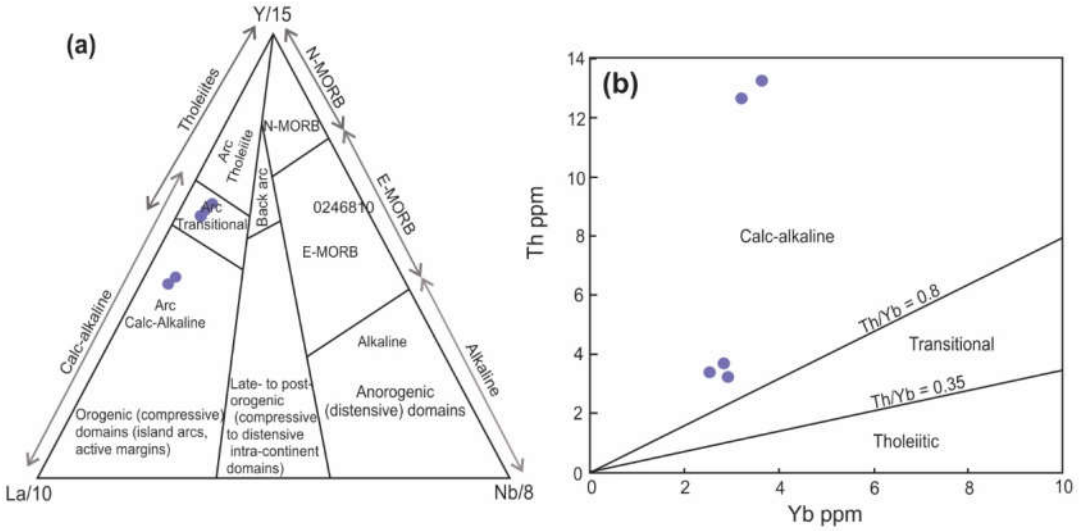

Figure 6.12 Tectonic discrimination diagrams for the high-grade gneiss; (a) Y-La-Nb ternary diagram (after [336]) illustrating orogenic affinity, and both diagram show all the samples belong to Calc-alkaline nature of basalt, (b) Th vs Yb bivariant plot (after [184]).

Table 6.1 Whole-rock geochemistry data for Daltonganj mafic granulites.

Sample	MM-12	S-1	D-8	K-1	RP-1	RP-4
SiO_2	48.96	48.86	48.95	48.99	48.91	48.98
Al_2O_3	14.68	13.99	13.55	13.8	13.03	13.75
TiO_2	1.07	1.87	2.04	1.11	3.21	1.75
Fe_2O_3	12.57	13.45	14.52	13.88	17.77	14.1
MnO	0.12	0.19	0.21	0.18	0.21	0.19
MgO	6.89	6.93	5.87	8.24	4.41	7.55
CaO	9.69	9.59	8.27	9.46	7.81	8.85
Na_2O	2.86	2.6	2.73	2.21	2.73	2.74
K_2O	0.85	1.03	1.74	0.71	0.43	1.25
P_2O_5	0.17	0.83	0.67	0.41	0.41	0.52
LOI	1.79	0.72	1.42	1.24	1.48	0.58
Total	99.65	100.06	99.97	100.23	100.4	100.26
V	207	262	317	194	764	786
Cr	254	338	117	447	41	45
Co	47	46	49	48	62	65
Ni	159	93	48	108	51	53
Cu	57	45	32	51	64	71
Zn	330	229	366	153	364	382
Rb	18	22	66	17	5.6	5.6
Sr	262	404	319	285	100	103
Zr	197	318	342	145	368	385
Nb	3.8	8.2	10.6	4.5	11.7	12.6
Mo	0.8	2.5	1.1	0.7	0.8	0.8
Cd	0.1	0.2	0.5	0.1	0.4	0.4
La	11.6	47	52	29.4	31.7	35
Ce	24.1	106	117	62	74	75
Pr	3.0	13.2	14.0	7.5	9.5	10.2
Nd	12.3	54.6	57.4	29.9	41	45
Sm	2.8	10.7	12.2	5.5	10.7	9.9
Eu	1.3	2.9	2.5	1.6	2.4	2.6
Gd	3.3	12.0	13.7	6.3	14.1	15.0
Dy	2.9	8.4	11.4	4.5	15	14.9
Ho	0.6	1.6	2.3	0.9	3.0	3.0
Er	1.6	4.7	6.8	2.5	9.4	9.7
Tm	0.2	0.6	0.9	0.4	1.3	1.3
Yb	1.7	3.8	6.1	2.4	8.6	8.2
Lu	0.3	0.5	0.9	0.4	1.2	1.2
Hf	15.8	27	16.4	3.4	20.5	21.0
Ta	4.6	6.8	6.1	6.9	4.6	4.9
Pb	7.5	11.	11.6	9.0	10.4	11.5
Th	1.5	4.6	9.4	5.5	7.0	6.6
U	0.4	0.8	2.4	1.0	3.2	3.3
Y	15.8	37.2	42.4	23.1	65	34.2
$(La/Lu)_N$	4.97	9.45	6.35	9.00	2.81	2.86

Table 6.2 Whole-rock geochemistry data for Daltonganj Pelitic granulites.

Sample	S-9	K-4	K-10	D-12	K-1	D-7	D-3
SiO_2	56.12	55.81	55.26	57.19	58.9	60.37	61.64
Al_2O_3	18.82	19.39	16.01	17.24	14.6	17.62	17.67
TiO_2	1.23	1.17	1.55	1.03	0.8	0.72	0.42
Fe_2O_3	8.57	9.05	8.79	8.94	9.7	7.83	7.42
MnO	0.17	0.19	0.18	0.17	0.19	0.14	0.12
MgO	1.11	1.17	5.06	2.08	2.4	2.3	2.53
CaO	5.68	5.86	8.67	5.68	5.8	1.42	1.31
Na_2O	2.12	2.56	0.23	1.41	0.4	2.35	2.1
K_2O	3.56	2.88	1.85	3.42	2.9	4.7	5.01
P_2O_5	0.67	0.53	0.51	0.46	0.4	0.34	0.21
Total	98.05	98.61	98.11	97.62	96.09	97.79	98.43
V	8.5	14.4	338	124	230	27	27
Cr	17.8	17.3	275	75	46	18	18
Co	6.8	6.8	51	19.5	29	4.7	4.7
Ni	10.7	9.7	93	27.5	17	8.0	8.3
Cu	8.5	7.4	39	13.8	12	2.6	2.6
Zn	242	221	264	195	151	98	97
Rb	73	45	15.6	63	68	164	164
Sr	1040	1029	375	625	258	419	421
Zr	263	124	355	295	72	649	658
Nb	6.4	7.9	4.8	6.1	8.1	3.2	3.3
Mo	1.6	0.5	0.2	0.5	0.5	0.3	0.3
Cd	0.4	0.5	0.2	0.3	0.1	0.4	0.4
La	113	78.3	30.4	121	53	392	382
Ce	228	145	66	175	119	797	818
Pr	25	17	8.3	23	14.1	72	71
Nd	100	66.9	34	98	61	240	238
Sm	16	11.4	6.8	14	14	27	27
Eu	15	10	1.9	6.5	2.4	5.6	5.6
Gd	17	12.8	8.0	17.5	16	30	30.5
Dy	8.9	6.9	5.9	8.5	12.7	6.9	7.1
Ho	1.7	1.3	1.1	1.0	2.4	1.2	1.2
Er	4.8	3.9	3.2	3.5	7.2	3.1	3.1
Tm	0.6	0.5	0.5	0.6	1.0	0.4	0.4
Yb	4.4	3.5	2.9	3.6	6.6	3.1	3.0
Lu	0.7	0.6	0.4	0.5	0.9	0.5	0.5
Hf	27.5	6.3	17.4	17.5	3.2	26	24.8
Ta	5.9	6.2	7.9	6.8	7.9	5.2	5.2
Pb	22.	21.9	10.3	20.2	18	38	37
Th	9.8	12.8	3.2	25.5	22	55	55
U	4.7	4.1	0.5	4.2	4.6	2.7	2.7
Y	84	65	62	54	60	45	43

Table 6.3 Whole-rock geochemistry data for high-grade gneiss from Daltonganj, CGGC.

	Grt-crd-amp gneiss			Grt-opx-amp gneiss	
	D7b	**D8a**	**R-91-96**	**K4a**	**R-91-97**
SiO_2	49.58	49.78	50.01	54.87	55.46
Al_2O_3	13.31	12.58	12.87	14.58	14.91
TiO_2	0.31	0.38	0.36	0.90	0.82
Fe_2O_3	17.31	16.54	15.68	10.86	11.26
MnO	0.06	0.06	0.04	0.03	0.06
MgO	13.32	14.56	14.87	10.89	9.71
CaO	1.26	1.36	1.58	2.54	2.80
Na_2O	0.81	0.28	0.71	0.78	0.66
K_2O	0.87	0.63	0.83	0.98	0.91
P_2O_5	0.29	0.31	0.27	0.36	0.38
Total	**97.12**	**96.48**	**97.22**	**96.79**	**96.97**
V	330	340	335	15	15
Cr	257	268	280	19	18
Co	60	52	53	6.2	6.6
Ni	88	92	96	10.3	9.7
Cu	36	40	41	8.6	7.6
Zn	258	266	273	236	226
Rb	14.6	16	16	51	46
Sr	384	371	381	1142	1070
Zr	362	352	362	152	126
Nb	4.6	4.8	5.1	8.6	7.9
Mo	0.2	0.2	0.1	0.4	0.5
Cd	0.3	0.3	0.3	0.5	0.6
La	29	31.2	32.1	81.3	80
Ce	65	66	67	154	150
Pr	7.9	8.6	8.6	19	18
Nd	34	35	35	71	69
Sm	6.9	6.6	6.8	13	12
Eu	1.8	1.9	1.8	12	11
Gd	7.7	8.2	8.5	13	13
Dy	6.2	5.8	5.7	7.3	6.6
Ho	1.0	1.2	1.1	1.7	1.3
Er	3.3	3.3	3.1	3.7	3.4
Tm	0.4	0.5	0.4	0.6	0.5
Yb	2.9	3.0	2.6	3.7	3.2
Lu	0.5	0.5	0.4	0.6	0.6
Hf	17.6	17.6	18.2	6.4	6.6
Ta	7.6	7.7	8.2	6.0	6.2
Pb	9.9	10.5	10.7	22.6	21.5
Th	3.5	3.2	3.2	13.2	12.6
U	0.5	0.5	0.5	4.5	4.2
Y	62	64	62.2	68	65
La_N/Lu_N	7.2	7.6	9.0	15.9	17.9
Eu_N/Eu_N*	0.7	0.8	0.7	2.9	2.8